IDENTIFICATION OF RETENTION AREAS USING AIRBORNE LIDAR DATA. A CASE STUDY FROM CENTRAL SWEDEN

***Jakub SEIDL*[1,2]**

DOI: 10.21163/GT_2023.182.12

ABSTRACT :
This paper presents a method for identifying retention areas in forest stands using publicly available ALS (Aerial Laser Scanning) data. Retention areas/trees are the cause of large inaccuracies in compartmental timber volume calculations when updated with remote sensing data. Tree height was selected as the most explanatory parameter for identification. The calculation of the threshold value for each compartment was based on data from the FMS (Forest Management System) or on the evaluation of the statistical distribution of LiDAR data in the compartment. The calculation was applied directly to the 3D point cloud, where points with the corresponding height were classified and processed into the resulting vector layer. Both methods were tested and validated on a reference dataset. The statistical approach proved to be more reliable (OA 89%) due to frequent errors or outdated data in the FMS (OA 82%). After removing dead retention trees (standing tree torsos) from the validation dataset, the OA of both methods increased (FMS approach 90%, statistical approach 94%).

Key-words: *ALS, LiDAR, Retention trees,* Forest *Management System, Sweden*

1. INTRODUCTION

With the increasing emphasis on biodiversity and sustainability, new approaches and practices have been introduced in various sectors. Forestry is undoubtedly one of them. As timber production can conflict with conservation objectives, a new concept of retention forestry (Beese et al., 2019) has been incorporated into the forest management system (Gustafsson et al., 2020). The aim is to promote biodiversity directly during timber harvesting. Retention is understood as a single tree or group of trees set aside in a logged area because it provides a home for different types of organisms (insects, fungi, etc.). They have become common practice in Scandinavian countries (Finland, Sweden, Norway) since the late 1990s and are included in national legislation and certification standards (Gustafsson et al., 2010).

Since the forest fulfills multiple roles (productive, ecological) a long-term management plan is needed to enhance or preserve it. For more detailed planning additional forest stands stratification is done (PEFC, 2016). Those areas are called compartments and present relatively homogeneous areas, which are then managed separately to achieve specific goals. For each compartment, a detailed description is provided including information about age, area, forestry objective, tree species distribution, volume, etc. These days, compartments are usually constructed with the usage of remote sensing data such as aerial or satellite images (Poso et al., 1987).

[1] *Stora Enso IT, Stora Enso Wood Products Ždírec s.r.o., Nová Karolina Park, 702 00, Ostrava, Czech Republic, jakub.seidl@storaenso.com*
[2] *Department of Geoinformatics, Faculty of Mining and Geology, VSB – Technical University of Ostrava, , Ostrava, Czech Republic, jakub.seidl@vsb.cz*

Forest inventory and monitoring benefit from new technologies. These make it possible to cover large areas and obtain important information on forest stands or even individual trees with less cost and effort required by traditional methods. An example of these technologies is Light Detection and Ranging (LiDAR, Pitman et al., 2004; Wandinger, 2005). Its ability to penetrate the tree canopy makes this technology almost ideal for forest mapping. There are multiple areas in forestry where LiDAR data are used these days. One of those is forest inventory and monitoring which usually incorporate techniques for tree detection, and calculation of their characteristics like height, volume (Hyyppa et al., 2001; Popescu et al., 2003; Andersen et al., 2004; Dalponte et al., 2016; Cao et al., 2016), or species classification (Heinzel et al., 2011; Yao et al., 2012). Other areas like forest ecology are interested in deriving information about biomass (Zhao et al., 2009; Gleason et al., 2012) or forest canopy structure (Zhao et al., 2011; Wang et al., 2008). Harvesting operations can also benefit from LiDAR-derived DTM that can be utilized as input for routing of forwarders (Holmström et al., 2023) or optimization of landings (Flisberg et al., 2022) to improve work efficiency and minimize environmental impact.

Regarding the tree parameters that can be derived from LiDAR data, two main approaches are usually distinguished: ABA (Area Based Approach) which is an estimate of selected parameters in some aggregation unit, and ITD (Individual Tree Detection) where all trees are tracked individually. Various techniques are utilized for ITD, such as the Watershed algorithm (Wu et al., 2019) and methods using Local Maxima Identification (Hyyppa et al., 2001), Polynominal Fitting Method (Cao et al., 2016), Individual Tree Crown Segmentation (Dalponte et al., 2016), and Point Cloud Segmentation (Li et al., 2012). Other methods use deep/machine learning (Chen et al., 2021) or graph theory (Strîmbu et al., 2015), or a combination of those methods where the result of one method serves as input into another (Wu et al., 2019).

Only a single study (Hardenbol et al., 2022) so far has dealt with the identification and classification of retention trees. The study used the ITD approach to identify and classify retention trees on ALS (Aerial Laser Scanning) data with a density of 5 points/m^2 in combination with not rectified CIR (color-infrared) aerial images in Finland. The basis of the ITD was CHM (Canopy Height Model) smoothing and local maxima detection in moving fixed size window. Then, tree crown boundaries were identified with the Watershed algorithm, and a height threshold was applied to keep only retention trees. The study reached a detection rate of 83.8% for living trees and 41.7% for dead trees.

This paper presents novel methods to identify retention areas using low-resolution ALS (Aerial Laser Scanning) data with a density around 2 points/m^2. Two methods are presented and evaluated. Both are based on ABA since forest retention is not only consisting of selected trees left after harvest but also complete small intact forest areas (Gustafsson et al., 2020). The objective of the presented work was:

i) to create a solution for identifying retention areas from publicly available data
ii) solution must be suitable for large areas using standard hardware

Currently, no dataset on retention areas is publicly available, although they can be beneficial for biodiversity applications and increase data accuracy in the forest management system. These systems typically include dominant tree height values at the compartment level, and retention areas can strongly influence them since the retention is usually much higher than the productivity layer.

2. DATA AND METHODS

2.1 Used data

Because of availability, sufficient detail, and coverage, publicly available LiDAR dataset from Lantmäteriet (https://www.lantmateriet.se/) was used as source data. Dataset covers the whole of Sweden with a minimum point density of 0.5 points/m^2 for all scanned surfaces and a minimum point density of 1.0 points/m^2 in forest areas, decreasing to 0.25 points/m^2 in bare mountains.

The height of flight from which scanning was realized ranged from 1700 to 2300 m above sea level (4000 m in mountains). The data acquisition was performed with a maximum scanning angle of ±20° and a lateral overlap of 10 to 20%. Absolute positional accuracy for open flat hard surfaces was 0.1 m in height and 0.3 m in plane. The data come pre-processed and classified into four categories (land, water, bridge, unclassified) and follow the SS-EN ISO 16157:2013 standard Geographic information - Data quality (Lantmäteriet, 2022).

Two areas (AOI 1, AOI 2) in Sweden (Norra Sverige, Dalarnas Län) were selected for testing the approach (**Fig. 1**). Both together cover approximately 250 km^2 and contain approximately 900 forest units less than 30 years old (see **Table 1** for more detailed information) which in total covers around 55 km^2. The main reason for age restriction is the fact, that retention forestry was implemented in the early 1990s, and therefore is no sense in processing older data. The point density was approximately 2.7 points/m^2 for both selected areas thus adequate for tree detection (Kaartinen et al. (2012) state sufficient point density for grown-up trees as 2 p/m^2).

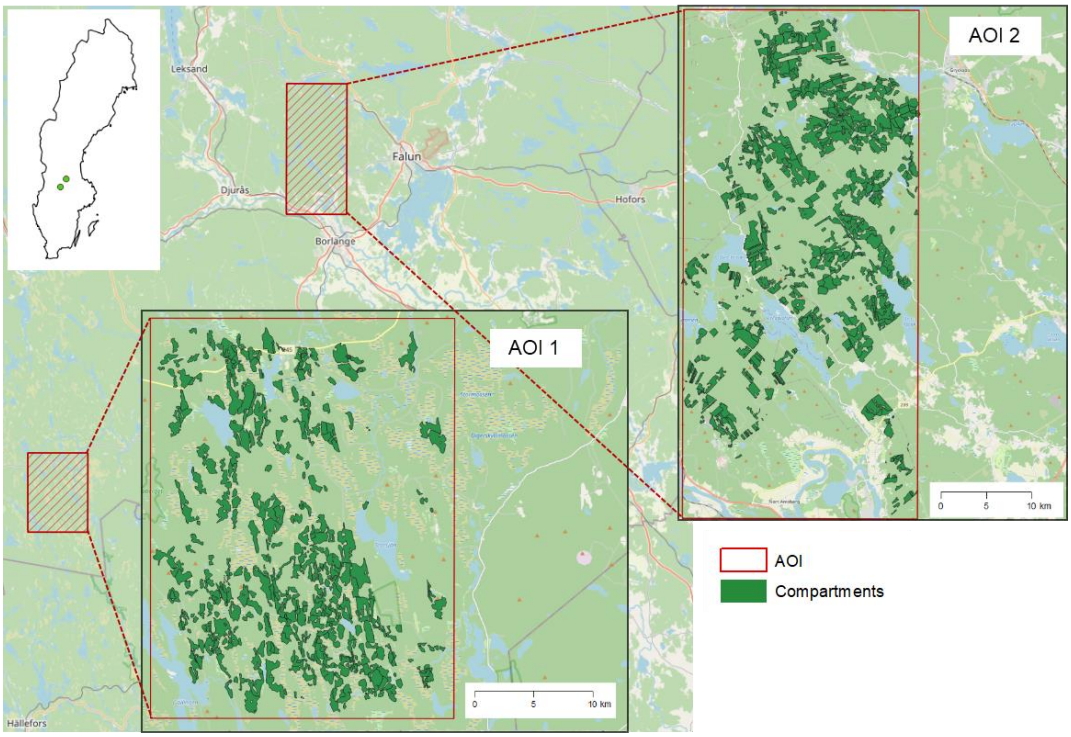

Fig. 1. Map of selected test areas.

Table 1.

Test area basic information.

	AOI 1	**AOI 2**
Area size (km2)	78 km2	189 km2
Number of compartments	249	668
Compartment coverage (km2)	22.7	34.5
Mean compartment size (km2)	0.07	0.05
Year of sensing	2021	2020

2.2. Retention areas identification

To stratify the forest, forest compartments were used to divide the forest into relatively homogeneous areas. The main assumption of the presented approach was that trees in retention areas should be significantly higher than other young trees in the forest compartment (production layer). Therefore, a simple height threshold for the whole compartment was defined to detect retention. To ensure that all retention trees are significantly taller than the production layer and thus identifiable in the LiDAR data, only stands younger than 30 years were selected. Two different approaches were then used (described in the processing section) and the results were validated.

It was decided to implement both approaches directly on the point cloud data (**Fig. 2**) instead of using techniques to identify retention on the CHM (Canopy Height Model) (Hardenbol et al., 2022). The main reason was that the point cloud data allowed us to obtain the number of points in each cell and thus omit cells with significant enough height but low point counts. These could potentially also be retention regions but with much lower reliability resulting from the low number of laser pulse measurements.

The whole calculation process was implemented in Python 3.10.8 (https://www.python.org/) with the libraries Numpy 1.22.3 (https://numpy.org/), Laspy 2.3.0 (https://laspy.readthedocs.io/), GDAL 3.5.1 (https://gdal.org/), Shapely 1.8.2 (https://shapely.readthedocs.io/), and PDAL 3.1.2 (https://pdal.io/en/latest/). The first step of the workflow is to crop the LiDAR point cloud data to the extent of the given forest compartment or another stratification layer to assure some level of forest homogeneity. The compartment geometry was converted from ESRI Shapefile to JSON format to be readable by the PDAL library. Then, for all points, the Z coordinate values were normalized to HAG (Height Above Ground) based on the distance of a particular point from the ground. The ground was interpolated from points classified as ground. The next step was classifying points representing retention. For this purpose, minimum tree height thresholds were calculated separately for each forest compartment. Two methods were used. The first one used data from the forest management system and was based on the information of the expected DOM (DOMinant tree height) in the forest compartment. Based on interviews with expert forest managers, it was decided to calculate the threshold as the expected DOM + 70%. DOM itself is usually calculated as the average height of the trees with the largest diameter at breast height (Kangas et al., 2011). The 70% enlargement should guarantee that all trees higher than that are true retention.

The second method was based on a statistical approach whereby retention was identified by statistically different heights compared to other points in the compartment that were not classified as ground. To deal with the possible different distribution of data in the compartments, the height values (x) were transformed into z-score values with the usage of PDAL *filters.assign* function which enables setting the filtering rule for a specific dimension of the point cloud that is applied to all points parsed as input to the function. The nature of the z-score implies that a higher value means that the value is less likely to come from a chance. Therefore z-score (Z) values greater than 3 (p-value = 0.0013) were considered statistically significant differences (three standard deviations (σ) away from the mean (μ)) and classified as potential retention:

$$Z = \frac{x - \mu}{\sigma} \tag{1}$$

where:

Z = the z-score
x = the height values
μ = the mean
σ = the standard deviations

This approach was chosen to evaluate the possibility of identifying retention areas in localities where forest management system DOM heights are not available.

Right after, points assigned to the retention class were converted into a two-band raster with a 2 m cell size (band 1: maximum height; band 2: number of points). With these data, a new Boolean raster was created (1: retention; 0: other). The number 1 was assigned to cells whose values were calculated from a sufficient number of points (at least 4 in a cell) or had a sufficient HAG value relative to the other retention areas in that compartment.

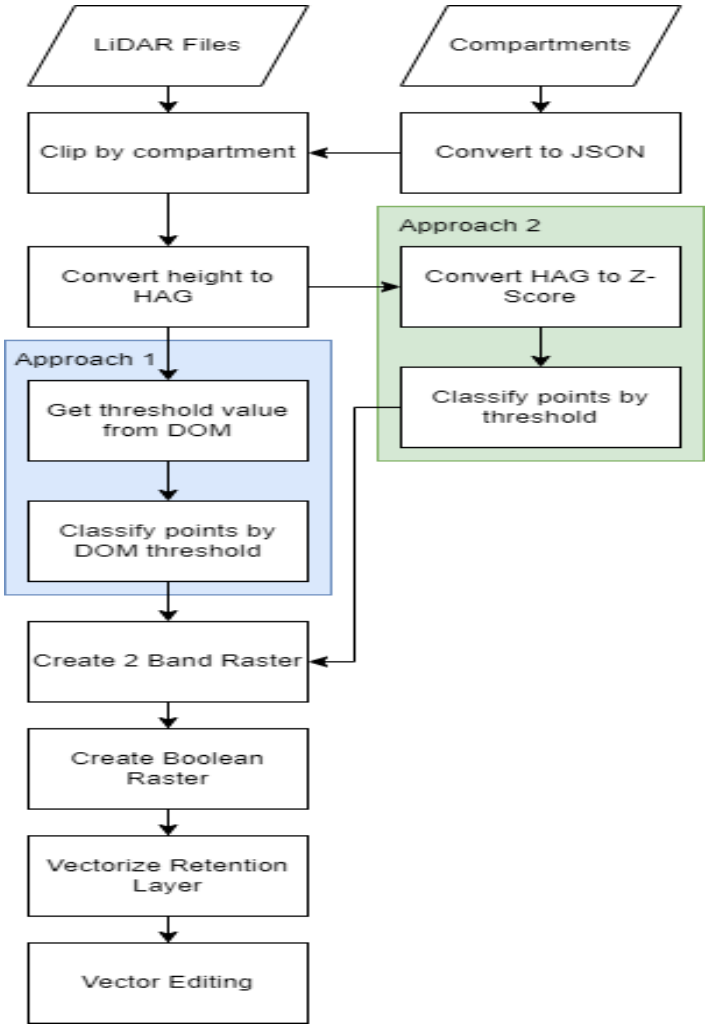

Fig. 2. Process schema.

In the last step, the Boolean raster was polygonized, and the following polygons were adjusted:

1) polygons smaller than 4 m^2 were removed to prevent false positives originating from overgrown vegetation (solo branches, etc.) or noise in the data;
2) polygons touching the forest compartment boundary were marked, to avoid errors originating from the boundary imprecision;
3) polygons that could potentially be solo trees were marked, based on the maximum area of the retention polygon and similarity to a circle (**Fig.3**). The area threshold was set to 160 m2 = 40 pix (approximately the area of the crown with a 7 m radius).

If the polygon satisfies the area condition a circle similarity was evaluated. The area of a circle with a diameter equal to the polygon's maximum distance was compared with the retention polygon area (the polygon must cover at least 65 % of the circle).

2.3. Validation

Validation was based on orthophotos with 16 cm GSD (Ground Sample Distance) acquired in the summer of 2022. Despite the problems arising from the time lag, these data are the most recent data suitable for validation. Given that field measurements from 2023 would extend the time gap. Prominent retention trees standing in cleared areas or among young/low vegetation were marked by visual inspection in both areas and divided into two classes (tree, dead tree). All trees without green branches or without visible branches at all were considered dead since the orthophotos were captured in the middle of vegetation season. Tree shadows were very useful in this case, as can be seen in **Figure 4.** Marking of reference trees was done before the retention areas processing, therefore the reference dataset was not influenced by prior knowledge of the process result.

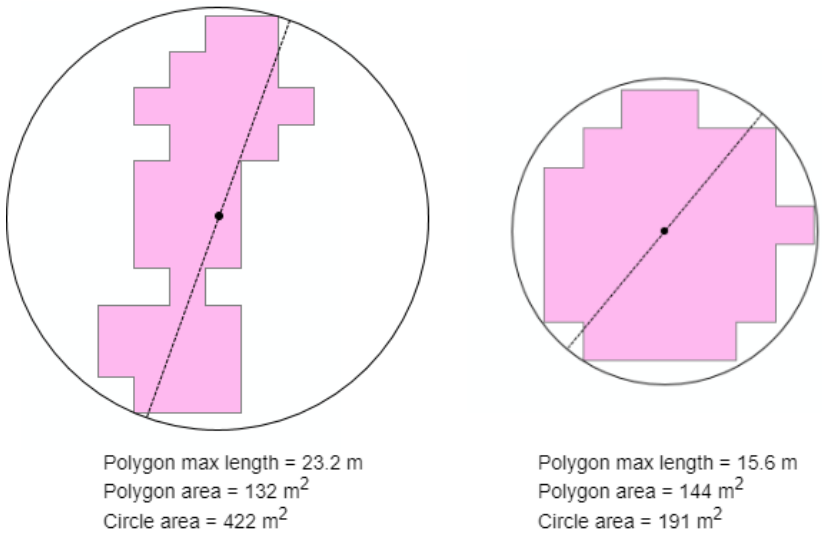

Fig. 3. Retention polygons comparison to area of circle where diameter is equal to maximum distance in given polygon.

Because of imprecision in compartment borders, all retention areas intersecting the border were not marked as a reference. Those areas were also removed from the outputs of both approaches. Polygon identification was used for a group of trees, otherwise, a point symbol was added. A straightforward validation method was then used: if the reference point feature laid within the retention polygon, then it was identified as correctly identified. In the case of reference polygons, the area coverage was compared. If the reference polygon was at least 80% covered by the retention polygon, it was considered correctly identified. In total, 874 reference points (790 trees; 94 torsos/dead trees) and 36 reference polygons were collected, covering a total area of 0.053 km2.

To evaluate the accuracy in greater detail, and calculate omission and commission errors, four compartments were selected in which all the retention trees were marked (based on orthophotos). Compartments were selected by the possibility to mark all retention with high certainty, also not to interfere with previously marked reference trees. In total, 89 additional trees were marked.

3. RESULTS

Firstly, an overall statistical evaluation of results coming from both approaches was done (**Table 2**). Mean and median values were very similar for both areas. There was a difference in max coverage value in both areas (more significant in Area 1). Overall statistical parameters were calculated in relation to compartments (**Table 3**). Approaches reached very similar mean retention coverage in compartments in both test areas (around 18% in AOI 1, and 10% in AOI 2). The major difference was identified in the maximum retention coverage in the compartment achieved by Approach 1 (used height threshold from FMS). This problem originated from data in FMS. A more detailed investigation was done in areas that were almost fully covered by retention identified by Approach 1, but Approach 2 (height threshold based on the statistical difference) did not identify any retention in those areas. This occurred only three times and was due to areas that had already been logged but were still fully grown forests on the LiDAR data. As can be seen in **Table 2**, Approach 2 in both areas delivered much more stratified results as can be derived from a higher number of identified retention areas, and lower mean and median values of area size. Despite that, the overall identified area was very similar for both approaches.

The next phase was validation with reference data collected from orthophoto images, see Section 2.3. The results are provided in **Table 4**. When all reference trees were included, Approach 1 showed an OA (Overall Accuracy) of 82 % and Approach 2 had an OA of 90%. Removal of trees classified as torsos/dead resulted in an improved overall accuracy of 89 % with Approach 1 and 94 % with Approach 2. The reason for that could be that the dead trees were quite often just torsos without branches therefore much smaller targets to be hit by a laser pulse.

Table 2.

Overall statistical parameters of identified retention areas (all retention polygons smaller than 4m^2 were removed).

	AOI 1		AOI 2	
	Approach 1	Approach 2	Approach 1	Approach 2
Max (m^2)	133300	12652	54180	18540
Mean (m^2)	164	117	138	120
Median (m^2)	44	40	52	44
Count	13380	17227	19519	23057
Total (km^2)	2.23	2.25	2.68	2.78

Table 3.

Overall statistical parameters of retention tree coverage for single compartment.

	AOI 1		AOI 2	
	Approach 1	Approach 2	Approach 1	Approach 2
Min (%)	0.08	0.00	0.00	0.00
Max (%)	0.93	0.53	0.64	0.78
Mean (%)	0.17	0.18	0.10	0.09
Median (%)	0.10	0.13	0.06	0.07

Table 4.

Retention tree identification overall accuracy.

		Approach 1		Approach 2	
	Tree count	Detected	OA	Detected	OA
Covered reference trees (all)	873	724	0.82	786	0.90
Ref. trees (no dead)	789	704	0.89	748	0.94

Figure 4 shows in a sample the result of the comparison between the retention areas (left) and solo retention trees (right) manually marked and retention layer.

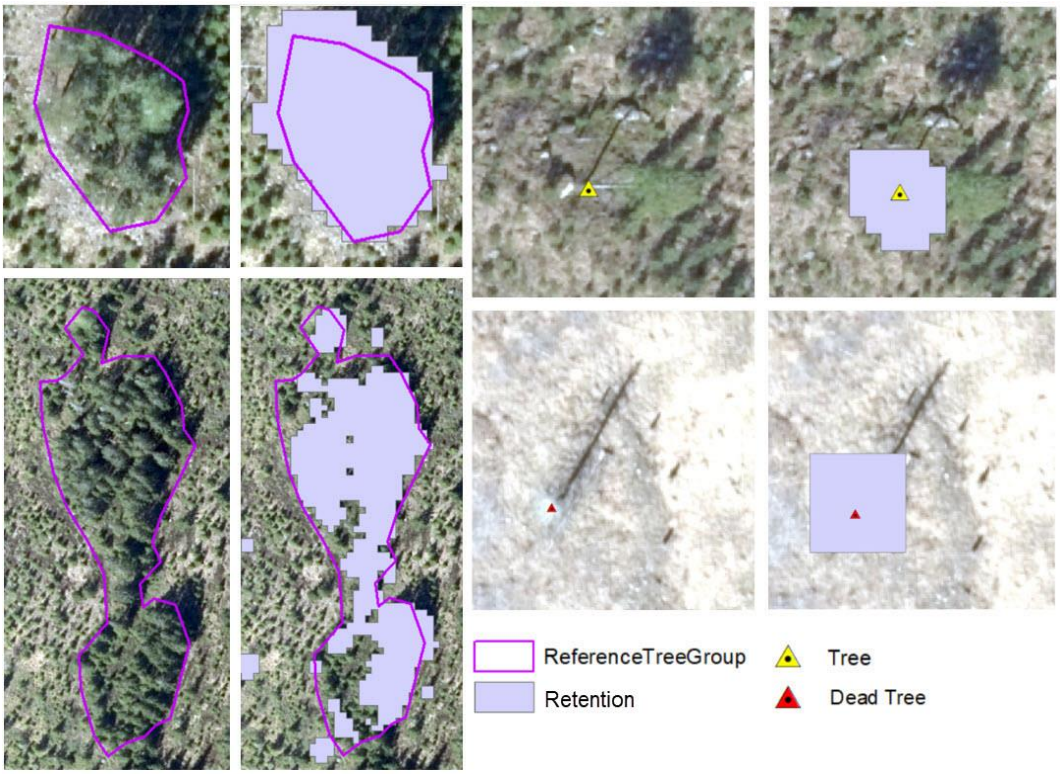

Fig. 4. Comparison of retention areas (left) and solo retention trees (right) manually marked and retention layer produced by presented approaches.

Based on the results given in **Table 5**, evaluating the accuracy of approaches in selected compartments, Approach 1 was more vulnerable to omission error.

Table 5.

Evaluation of error in compartments where all retention trees were marked as reference.

Approach 1	Number of trees	Correct	False Positive	Commission error	False Negative	Omission error
Compartment 1	33	31	1	0.03	2	0.06
Compartment 2	26	23	3	0.12	3	0.12
Compartment 3	17	15	0	0	2	0.14
Compartment 4	13	10	2	0.15	3	0.23
Total	**89**	**79**	**6**	**0.08**	**10**	**0.14**

Approach 2	Number of trees	Correct	False Positive	Commission error	False Negative	Omission error
Compartment 1	33	31	4	0.12	2	0.06
Compartment 2	26	25	5	0.19	1	0.04
Compartment 3	17	16	0	0	0	0
Compartment 4	13	11	4	0.30	2	0.15
Total	**89**	**83**	**13**	**0.15**	**5**	**0.06**

The main factor was most probably the threshold coming from FMS, therefore there was no direct relation to the data itself. As opposed to that Approach 2 resulted as more vulnerable to commission error. One possible explanation of the commission seems to be that trees fell in the time gap between orthophotos and LiDAR data capture. On multiple occasions, there were fallen trees that were still identifiable in LiDAR data but not marked on orthophotos (see **Fig. 5**).

Fig. 5. Commission error caused by trees fell between LiDAR data and orthophoto images.

Overall, (see **Fig. 5**) both retention area identification approaches delivered very similar results in many cases. This applies mostly to solo standing trees and dense groups of trees. The most divergent results were in areas of sparse retention vegetation areas inside clear-cut areas. Approach 1 with the threshold from FMS found only the taller trees in the area, while Approach 2 included also the lower part of the vegetation. This behavior was the result of differences in the bases of both applied approaches (**Fig. 6**).

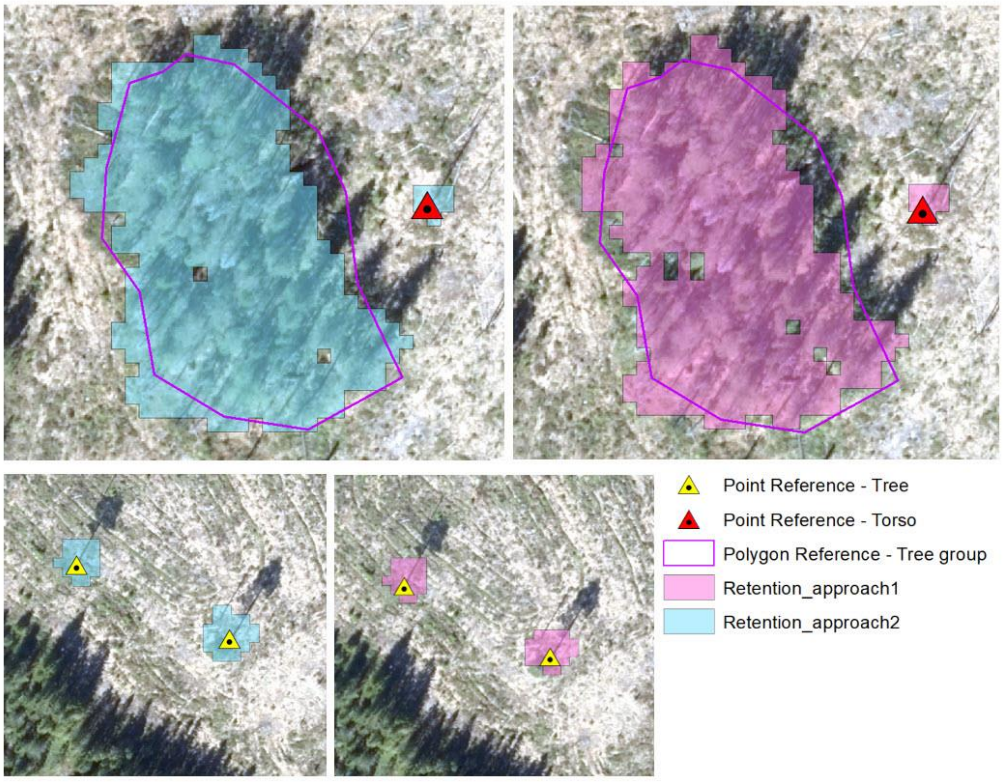

Fig. 6. Comparison of results of both presented approaches.

4. DISCUSSION

According to **Table 4** and **Table 5** given in the Results section, both proposed approaches achieved encouraging results despite some limitations. As was already mentioned, approaches were applied for forest stands younger than 30 years, where a significant difference in height between the production layer and potential retention is expected. Applying the same methods for older forests might result in an increased error therefore threshold calculation methods should be modified to minimize this. Also, a forest compartment layer is required on input. Such a layer is standardly available in forest management systems in countries all over the world. In case the forest compartment layer is not available, another stratification layer needs to be calculated (e.g. Watershed (Vincent et al., 1991), thresholding (Davis et al., 1975), region or edge-based methods (Gould et al., 2009; Wani et al., 1994; Fan, 2010; Angelina et al., 2012), etc.) and provided as input to the process.

To evaluate the robustness of the process a larger dataset covering more heterogeneous areas could be used. The validation results can be partly influenced by errors arising from reference data manual collection on orthophotos as mentioned in previous sections. Instead of them, precisely measured field data could be used, e.g. by applying GNSS Real-Time Kinematic (RTK, Teunissen and Motenbruck, 2017) or a similar approach for highly accurate positioning. Acquisition of both reference and ALS datasets should be done in a similar time period to capture the same situation in forests.

So far, only the Hardenbol et al. (2022) study dealt with the identification of retention trees. Their method was built on the ITD approach. In contrast to that, our methods utilize the ABA approach to minimize errors originating in not finding all individual trees in a scene, which could be challenging even with high-density LiDAR data. The ABA approach is also more in accordance with the goals of this paper, to identify the area covered by retention instead of identifying each retention tree likewise to keep the processing more computationally efficient. Our approaches were applied to sparser point cloud data than in the mentioned study and also did not use any additional remote sensing data. As well as in Hardenbol et al. (2022), dead trees, which are very difficult to detect with lower point cloud densities, had a significant effect on the accuracy of the presented approaches.

5. CONCLUSION

Information about retention areas in forest compartments is needed for a better understanding of overall forest conditions and for more precise forest management planning. The study presented two novel ABA methods for retention areas identification based on a low-density LiDAR point cloud from ALS. Both methods are easily applicable for computation over large areas while using a standard personal computer. During the validation, both proposed methods delivered promising results with 82% overall accuracy delivered by the first approach based on FMS data on input and 90% by the second approach based on statistical differences in height. As the second approach delivered slightly better performance and does not require additional data on the input, it can be recommended in overall. Since data from ALS with needed point density are publicly available in many countries over the world, there are no inhibitions present to apply the described methods for the creation of national retention areas datasets.

REFERENCES

Andersen, H.-E., McGaughey, R., Reutebuch, S. (2005) Estimating Forest canopy fuel parameters using LIDAR data. *Remote sensing of Environment*, 94 (4), 441-449.

Angelina, S., Suresh, L. P., Veni, S. H. K. (2012) Image segmentation based on genetic algorithm for region growth and region merging. In 2012 international conference on computing, electronics and electrical technologies (ICCEET), 970-974, Tamil, India, March 2012.

Beese, W. J., Deal, J., Dunsworth, B. G., Mitchell, S. J., Philpott, T. J. (2019) Two decades of variable retention in British Columbia: a review of its implementation and effectiveness for biodiversity conservation. *Ecological Processes*, 8 (1), 1-22.

Cao, L., Gao, S., Li, P., Yun, T., Shen, X., Ruan, H. (2016) Aboveground biomass estimation of individual trees in a coastal planted forest using full-waveform airborne laser scanning data. *Remote Sensing*, 8 (9), 729.

Chen, X., Jiang, K., Zhu, Y., Wang, X., & Yun, T. (2021). Individual tree crown segmentation directly from UAV-borne LiDAR data using the PointNet of deep learning. *Forests*, *12*(2), 131.

Dalponte, M., Coomes, D., A. (2016) Tree-centric mapping of forest carbon density from airborne laser scanning and hyperspectral data. *Methods in ecology and evolution*, 7 (10), 1236-1245.

Davis, L., S., Rosenfeld, A., Weska, J. S. (1975) Region extraction by averaging and thresholding. *IEEE transactions on systems, man, and cybernetics*, 3, 383-388.

Flisberg, P., Rönnqvist, M., Willén, E., Forsmark, V., & Davidsson, A. (2022) Optimized locations of landings in forest operations. *Canadian Journal of Forest Research*, *52*(1), 59-69.

Gleason, C. J., & Im, J. (2012) Forest biomass estimation from airborne LiDAR data using machine learning approaches. *Remote Sensing of Environment*, *125*, 80-91.

Gould, S., Gao, T., Koller, D. (2009) Region-based segmentation and object detection. *Advances in neural information processing systems*, 22.

Gustafsson, L., Bauhus, J., Asbeck, T., Augustynczik, A.L.D., Basile, M., Frey, J., Gutzat, F., Hanewinkel, M., Helbach, J., Jonker, M., Knuff, A., Messie,r C., Penner, J., Pyttel, P., Reif, A., Storch, F., Winiger, N., Winkel, G., Yousefpour, R., Storch, I. (2020) Retention as an integrated biodiversity conservation approach for continuous-cover forestry in Europe. *Ambio*, 49, 85-97.

Gustafsson, L., Kouki, J., Sverdrup-Thygeson, A. (2010) Tree retention as a conservation measure in clear-cut forests of northern Europe: a review of ecological consequences. *Scandinavian Journal of Forest Research*, 25 (4), 295-308.

Hardenbol, A. A., Korhonen, L., Kukkonen, M., Maltamo, M. (2022) Detection of standing retention trees in boreal forests with airborne laser scanning point clouds and multispectral imagery. *Methods in Ecology and Evolution*.

Heinzel, J., & Koch, B. (2011) Exploring full-waveform LiDAR parameters for tree species classification. *International Journal of Applied Earth Observation and Geoinformation*, *13*(1), 152-160.

Holmström, E., Nikander, J., Backman, J., Väätäinen, K., Uusitalo, J., & Jylhä, P. (2023) A multi-objective optimization strategy for timber forwarding in cut-to-length harvesting operations. *International Journal of Forest Engineering*, *34*(2), 267-283.

Hyyppä, J., Kelle, O., Lehikoinen, M., Inkinen, M. (2001) A segmentation-based method to retrieve stem volume estimates from 3-D tree height models produced by laser scanners. *IEEE Transactions on geoscience and remote sensing*, 39 (5), 969-975.

Kaartinen, H., Hyyppä, J., Yu, X., Vastaranta, M., Hyyppä, H., Kukko, A., Holopainen, M., Heipke, C., Hirschmugl, M., Morsdorf, F., Næsset, E., Pitkänen, J., Popescu, S., Solberg, S., Wolf, B.M., Wu, J.-C. (2012) An international comparison of individual tree detection and extraction using airborne laser scanning. *Remote Sensing*, 4 (4), 950-974.

Kangas A., Päivinen R., Holopainen M., Maltamo M. (2011). Silva Carelica 40. Metsänmittaus ja kartoitus. [Forest mensuration and mapping]. University of Eastern Finland, School of Forest Sciences. 210 p.

Lantmäteriet, (2022-04-05), *Product Description Laser data Download, NH*, Available online at: https://www.lantmateriet.se/globalassets/geodata/geodataprodukter/hojddata/e_pb_laserdata_nedladdning_nh.pdf, (Accessed: May 1, 2023)

Lantmäteriet, (2022-04-05), *Quality Description Laser data*, Available online at: https://www.lantmateriet.se/globalassets/geodata/geodataprodukter/hojddata/quality_description_lidar.pdf, (Accessed: May 4, 2023)

Li, W., Guo, Q., Jakubowski, M. K., & Kelly, M. (2012). A new method for segmenting individual trees from the lidar point cloud. *Photogrammetric Engineering & Remote Sensing*, *78*(1), 75-84.

PEFC, (2016-04-20), Programmer for The Endorsement of Forest Certification Sweden Forest Standard, PEFC SWE 002:4, Available online at: https://cdn.pefc.org/pefc.se/media/2021-02/49cc8975-4e4e-4f6e-9c95-37f4829f869f/2c1bd611-0b7f-5c7a-b76d-137e70cfdf42.pdf, (Accessed: May 4, 2023)

Pitman, J., Duncan, A., Stubbs, D., Sigler, R., Kendrick, R., Smith, E., Mason, J., Delory, G., Lipps, J. H., Manga, M., Graham, J., De Pater, I., Reiboldt, S., Bierhaus, E., Dalton, J. B., Fienup, J., Yu, J. (2004) Remote sensing space science enabled by the multiple instrument distributed aperture sensor (MIDAS) concept. In: Proceedings of SPIE - The International Society for Optical Engineering, 5555, pp. 301 - 311.

Popescu, S., C., Wynne, R. H., Nelson, R. F. (2003) Measuring individual tree crown diameter with lidar and assessing its influence on estimating forest volume and biomass. *Canadian journal of remote sensing*, 29 (5), 564-577.

Poso, S., Paananen, R., Similä, M. (1987) Forest inventory by compartments using satellite imagery. *Silva Fennica*, 21 (1), 69-94.

Strîmbu, V. F., & Strîmbu, B. M. (2015). A graph-based segmentation algorithm for tree crown extraction using airborne LiDAR data. *ISPRS Journal of Photogrammetry and Remote Sensing*, *104*, 30-43.

Swedish Standards Institute. (2013) Information and documentation -- Principles and functional requirements for records in electronic office environments (SS-EN ISO 16157:2013). Stockholm, Sweden: Swedish Standards Institute.

Tang, J. (2010) A color image segmentation algorithm based on region growing. In: 2010 2nd international conference on computer engineering and technology, pp. V6634-V6637, Chengdu, China, April 2010.

Teunissen, P. J. G., Montenbruck, O., (ed.). (2017) Springer handbook of global navigation satellite systems. Cham, Switzerland: *Springer International Publishing*.

Vincent, L., Soille, P. (1991) Watersheds in digital spaces: An efficient algorithm based on immersion simulations. *IEEE Transactions on Pattern Analysis and Machine Intelligence*, 13 (6), 583–598.

Wandinger, U. (2005) Introduction to Lidar. In: Weitkamp, C. (eds) Lidar. Springer Series in Optical Sciences, 102, Springer, New York, USA.

Wang, Y., Weinacker, H., & Koch, B. (2008) A lidar point cloud-based procedure for vertical canopy structure analysis and 3D single tree modelling in forest. *Sensors*, *8*(6), 3938-3951.

Wani, M. A., Batchelor, B., G. (1994) Edge-region-based segmentation of range images. *IEEE Transactions on Pattern Analysis and Machine Intelligence*, 16 (3), 314-319.

Wu, X., Shen, X., Cao, L., Wang, G., Cao, F. (2019) Assessment of individual tree detection and canopy cover estimation using unmanned aerial vehicle based light detection and ranging (UAV-LiDAR) data in planted forests. *Remote Sensing*, 11, (8), 908.

Yao, W., Krzystek, P., & Heurich, M. (2012) Tree species classification and estimation of stem volume and DBH based on single tree extraction by exploiting airborne full-waveform LiDAR data. *Remote Sensing of Environment*, *123*, 368-380.

Zhao, K., Popescu, S., & Nelson, R. (2009) Lidar remote sensing of forest biomass: A scale-invariant estimation approach using airborne lasers. *Remote Sensing of Environment*, *113*(1), 182-196.

Zhao, K., Popescu, S., Meng, X., Pang, Y., & Agca, M. (2011) Characterizing Forest canopy structure with lidar composite metrics and machine learning. *Remote Sensing of Environment*, *115*(8), 1978-1996.